Итоговый отчет по проекту КМПП-2015
«Дизайн высокотемпературных регенерируемых сорбентов CO_2»

Владимир Сергеевич Деревщиков, Виктория Сергеевна Семейкина,
Евгений Геннадьевич Малькович

Введение

В условиях роста потребления ископаемых топлив и обеспокоенности мирового сообщества растущими выбросами парниковых газов (CO_2) приоритетным направлением развития энергетики является рациональное использование энергоресурсов и развитие технологий, направленных на ограничение эмиссии углекислого газа. На сегодняшний день регенерируемые сорбенты CO_2 на основе оксида кальция рассматриваются в качестве перспективных материалов для связывания диоксида углерода в процессах очистки дымовых газов электростанций, ТЭЦ и процессах газификации биомассы с целью получения водорода для топливных элементов [1].

Основной проблемой использования сорбентов CO_2 является уменьшение их сорбционной емкости в циклах сорбция/регенерациия, происходящее вследствие спекания. Известно, что текстурные свойства поглотителей существенно влияют как на величину, так и на стабильность сорбционной емкости в циклах сорбции регенерации [2]. Для получения образцов сорбентов на основе CaO с различной пористой структурой используют ряд методов приготовления: прямое термическое разложение природных известняков, Ca-содержащих солей и гидроксидов, «мокрые» методики, в которых осаждаются частицы предшественника определенных размеров и форм, золь-гель метод, гидролиз алкосидов кальция и пламенный пиролиз. В указанных способах текстура поглотителя регулируется в основном химической природой предшественников и условиями синтеза [3].

В последние два десятилетия активное развитие получил подход к синтезу керамических материалов и катализаторов, в котором в образец для порообразования вводится темплат с заданными формой и размером частиц. После формирования и отвердения гранул частицы темплата удаляются, в результате чего образец приобретает требуемую пористую структуру, с заданным размером и объемом пор [4].

Мы полагаем, что темплатный подход позволит создать сорбенты CO_2 с оптимальной пористой структурой, способной обеспечит высокие эксплуатационные характеристики.

В целях оптимизации пористой структуры будет использовано математическое моделирование, основанное на методах вычислительной топологии [5].

Цель работы

Основной целью работы является целенаправленный синтез новых высокотемпературных сорбентов CO_2, обладающих высокой и стабильной сорбционной емкостью, и механической прочностью. В рамках работы планируется исследовать перспективы темплатного метода синтеза для приготовления сорбентов и др. пористых материалов и проверить применимость современных методов моделирования для расчета сорбционных свойств поглотителей.

Результаты выполнения работ по первому этапу проекта

В рамках первого этапа планировали провести синтез партии массивных хемосорбентов диоксида углерода на основе чистого CaO с использованием темплатного метода, и подробно изучить их текстурные и сорбционные свойства. В результате проделанной работы было обнаружено, что темплатный подход может быть использован в качестве прямого метода для формирования пористой структуры сорбентов на основе оксида кальция. Функция пористости, появляющейся в сорбенте в результате выжигания темплатного агента зависит не только от объема внесенного темплата, но и от размера исходных частиц, и температуры термообработки. Показано, что в случае частиц темплата с размером менее 1 мкм не удается провести диспергирование агломератов частиц до отдельных частиц обычными методами. В результате объем пор и средний размер пор, возникающие в носителе при выжигании темплата, превосходят расчетный объем пор, рассчитанный из данных по массе и плотности вносимого темплата. В случае частиц ≈ 1 мкм пористая структура сорбента практически полностью совпадает с расчетной. Сорбционные свойства синтезированных сорбентов четко указывают на то, что более развитая пористая структура позволяет обеспечить более высокую скорость десорбции диоксида углерода сорбентами, что является важным фактором для практического применения. Сорбенты, приготовленные с использованием темплата, обладали большей и более стабильной величиной сорбционной емкости, по сравнению с сорбентами, полученными бестемплатным способом (Рис. 1).

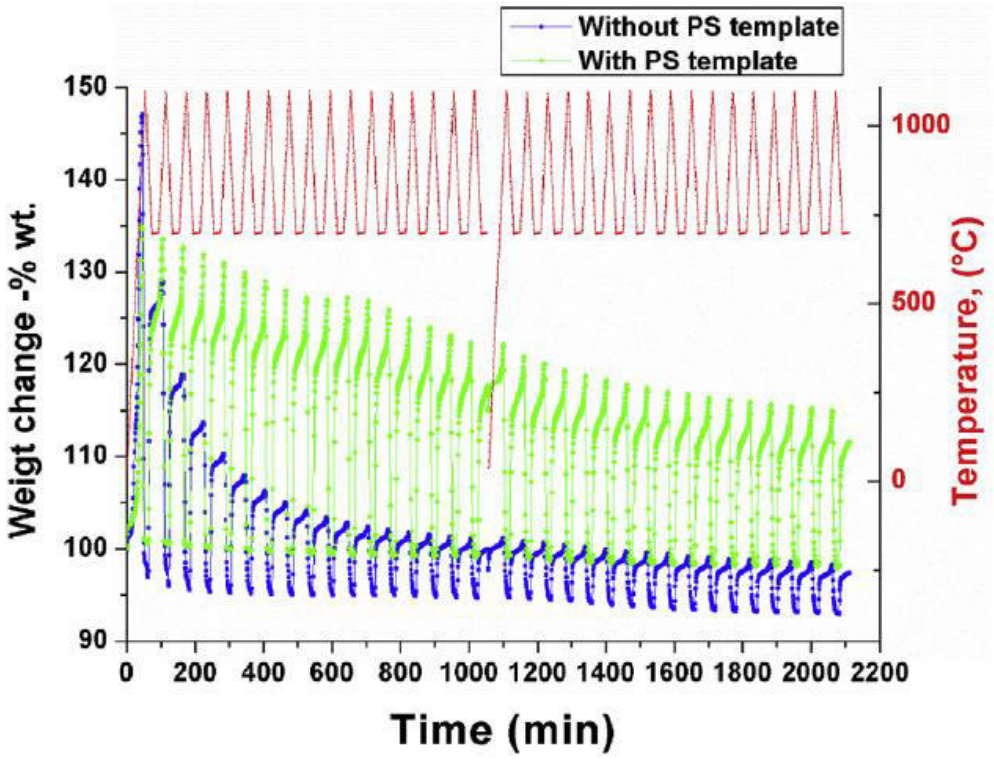

Рис. 1 Емкость сорбентов в циклах сорбции/регенерации.

Подробное описание синтеза и исследования свойств темплатных сорбентов приведены в публикации, приложенной к итоговому отчету.

Результаты работ по второму этапу проекта

Важной задачей при разработке новых высокотемпературных поглотителей является создание надежного инструмента прогнозирования свойств сорбентов, основанного на анализе экспериментальных условий и строения поглотителя. Существует обширный экспериментальный материал по изменению морфологических и сорбционных свойств сорбентов в процессе эксплуатации. На базе этих данных создано качественное описание механизма спекания CaO в циклах сорбции/ регенерации (Рис. 2.)[6].

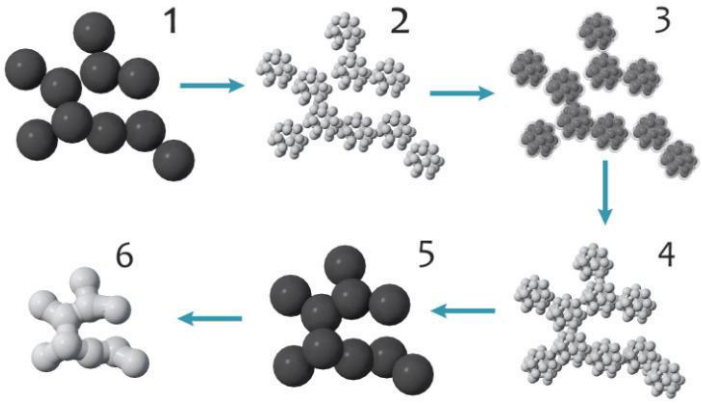

Рис. 2. Изменение текстуры сорбента в циклах сорбции/регенерации. (1-исходный сорбент, 2-сорбент после первой регенерации, 3- сорбент после первой сорбции, 4-сорбент после второй регенерации, 5- сорбент после n циклов сорбии, 6- сорбент после n циклов регенерации.

С другой стороны, математическое моделирование этих систем в процессе циклов сорбции/регенерации представлено в литературе полуэмпирическими зависимостями значения динамической емкости от номера цикла в виде степенных или экспоненциальных функций [2], которые не учитывают такие параметры, как продолжительность цикла сорбции/регенерации, текстуру адсорбента. Складывается ситуация, когда одно уравнение описывает одну экспериментальную кривую и не может быть применено при изменении условий эксперимента.

В данной работе нами была разработана модель, которая учитывает морфологию исходного сорбента, кинетику поглощения углекислого газа в циклах сорбции/регенерации при разных температурах. Ниже приведем краткое описание модели. Исходная система представляла собой случайную упаковку шаров, пористость и размер частиц которой соответствует экспериментальной [6]. Далее моделировался рост радиуса шаров во времени – чему в реальности соответствует рост слоя $CaCO_3$ на поверхности CaO в результате

топохимической реакции. Спекание системы моделировалось как сближение шаров в упаковке. Из практики известно, что увеличение продолжительности времени сорбции CO_2 (т.е. толщины слоя наросшего карбоната кальция) ускоряет спекание системы. Это было учтено в уравнении сближения частиц, которое было решено для системы двух частиц и распространено на всю систему шаров случайной упаковки. Итерационное решение уравнения позволило получить характеристики сближения шаров, далее рассчитать удельную поверхность образца и определить значение динамической емкости сорбента в циклах. Из рисунка 3 видно, что созданная модель позволяет предсказывать поведение системы с высокой достоверностью даже при изменении продолжительности стадий эксперимента.

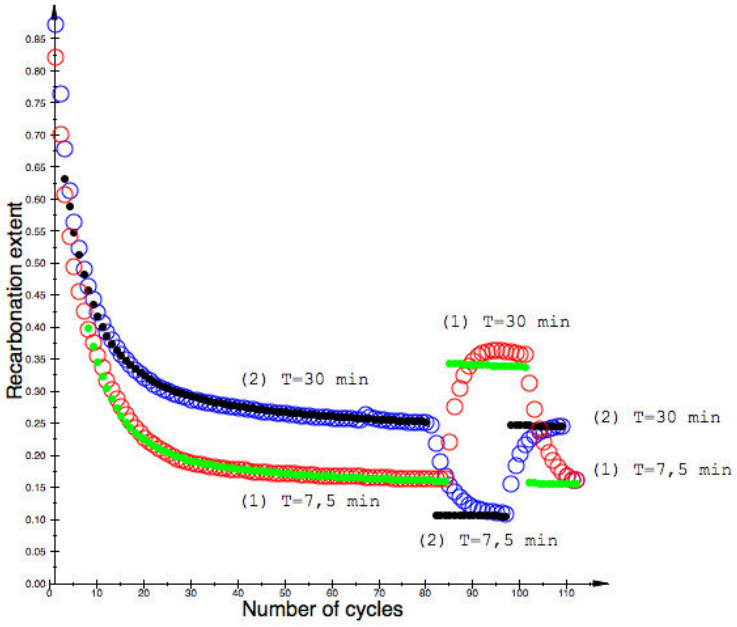

Рис. 3 Динамическая емкость по CO_2 сорбента в циклах (син., красн. - эксперимент; черн., зелен. - модель).

Подробное описание разработанной математической модели приведено в подготовленной публикации, приложенной к итоговому отчету.

Основные выводы

1. Темплатный метод синтеза позволяет напрямую формировать заданную макропористую структуру материала.
2. Развитая пористая структура позволяет обеспечить высокую скорость десорбции диоксида углерода сорбентами, что является важным фактором для их практического применения.
3. Сорбенты, приготовленные с использованием темплата, обладали большей и более стабильной величиной сорбционной динамической емкости по сравнению с образцами, приготовленными без темплата.

4. Была разработана математическая модель, учитывающая текстурные характеристики исходного сорбента, влияние кинетики реакции карбонизации и позволяющая прогнозировать значение динамической емкости и текстурных характеристик сорбента в циклах сорбции/регенерации разной продолжительности.
5. Проделанная работа позволила подтвердить перспективность выбранной темы исследований и послужит основанием для последующих работ по моделированию и синтезу новых материалов в будущем.

Публикации и доклады на конференциях, подготовленные в рамках проекта

1) Template technique for synthesis of CaO-based sorbents with designed macroporous structure / J. Bitar, V.S. Derevschikov,, A.G. Okunev, V.S. Semeykina, E.V. Parkhomchuk //Microporous Mesoporous Materials – 2016. – doi:10.1016/j.micromeso.2016.02.032.

2). Template technique for Synthesis of CaO-based sorbents // J. Bitar, V.S. Derevschikov,, A.G. Okunev, V.S. Semeykina, E.V. Parkhomchuk/ IMMS-9,Brisbane, Australia, 17~20 August 2015.

3) DESIGN OF CaO-BASED SORBENTS FOR CO2 SEPARATIONS // V.S. Derevschikov,, A.G. Okunev, V.S. Semeykina, E.V. Parkhomchuk/IMEC-17, Ramath-Gan, Israel, 1-2 Febraury 2016.

4) Evolution of Textural Properties of CaO-based Sorbents during Repetitive Sorption/Regeneration Cycles //Ya.V. Bazaikin, E.G. Malkovich, V.S. Derevschikov, A.I Lysikov and A. G. Okunev направлена в печать.

Использованная литература

[1] J. Wang, V. Manovic, Y. Wu, E.J. Anthony, CaO-based sorbents for capturing CO2 in clean energy proceses, Chem. Eng. Trans. 21 (2010) , pp. 643–648. doi:10.3303/CET1021108.

[2] D. Alvarez, J.C. Abanades, Pore-size and shape effects on the recarbonation performance of calcium oxide submitted to repeated calcination/recarbonation cycles, Energy and Fuels. 19 (2005), pp. 270–278. doi:10.1021/ef049864m.

[3] C. Luo, Y. Zheng, Y. Xu, N. Ding, Q. Shen, C. Zheng, Wet mixing combustion synthesis of CaO-based sorbents for high temperature cyclic CO_2 capture, Chem. Eng. J. 267 (2015), pp. 111–116. doi:10.1016/j.cej.2015.01.005.

[4] Brian T. Holland, Christopher F. Blanford, Andreas Stein Synthesis of Macroporous Minerals with Highly Ordered Three-Dimensional Arrays of Spheroidal Voids. Science 24 July 1998: Vol. 281 no. 5376), pp. 538-540.

[5] Daniela M. Ushizima, Dmitriy Morozov, Gunther H. Weber, Andrea G. C. Bianchi, James A. Sethian, E. Wes Bethel, Augmented Topological Descriptors of Pore Networks for Material Science IEEE Trans. Vis. Comput. Graph. (2012):Vol. 18(12), pp. 2041-2050.

[6] A. I. Lysikov, A. N.Salanov, A. G. Okunev, Change of CO_2 carrying capacity of CaO in isothermal recarbonation decomposition cycles. *Ind. Eng. Chem. Res.* (2007): Vol *46* (13), pp. 4633–4638.

Microporous and Mesoporous Materials xxx (2016) 1–6

Contents lists available at ScienceDirect

Microporous and Mesoporous Materials

journal homepage: www.elsevier.com/locate/micromeso

Template technique for synthesis of CaO-based sorbents with designed macroporous structure

Vladimir Derevschikov [a, b, c, *], Victoria Semeykina [a, b, c], Jasmine Bitar [b, d], Ekaterina Parkhomchuk [a, b, c], Alexey Okunev [b, a]

[a] Boreskov Institute of Catalysis, Pr. Lavrentieva 5, Novosibirsk 630090, Russia
[b] Novosibirsk State University, Pirogova Str. 2, Novosibirsk 630090, Russia
[c] Research and Educational Center for Energy Efficient Catalysis in Novosibirsk State University, Novosibirsk 630090, Russia
[d] ENSTA ParisTech, 828 Boulevard Des Maréchaux, 91120 Palaiseau, France

ARTICLE INFO

Article history:
Received 14 September 2015
Received in revised form
10 February 2016
Accepted 12 February 2016
Available online xxx

Keywords:
Carbon capture
Calcium oxide
Template
Porous structure
Regenerable sorbent

ABSTRACT

A polymeric template consisting of polystyrene microbeads was used to provide the macroporous structure of synthesized CaO-based sorbents. It was found that the pore size distribution of prepared and calcined sorbents drastically depends on the amount and particle size of the template used, as well as on the sorbent preparation conditions. The macroporous structure formed after the template removal significantly increases the rate of both recarbonation and decomposition reactions. The decomposition rate of the sorbent produced from a 40% templated composite was an order of magnitude higher than the rate of a reference sample produced in the absence of the template. In this way, the template approach seems to be a perspective technique to prepare CaO-based sorbents with enhanced recarbonation/decomposition performance.

1. Introduction

Emission of large amounts of CO_2 to the atmosphere, mostly as a by-product of burning fossil fuels in man-made processes, significantly contributes to the climate change [1,2]. The need to move toward a sustainable energy future motivates the search for new technologies to meet the ever-growing world energy demand. One of the options for reducing greenhouse gas emissions is the CO_2 capture and storage from large stationary sources [3–5] and during biomass gasification [6,7] by means of solid sorbents. Some studies on this topic suggest the use of calcium-based sorbents for the effective capture of CO_2 at high temperatures based on the reversibility of the reaction [8–11]:

$$CaO + CO_2 \leftrightarrow CaCO_3.$$

CaO-based sorbents exhibit nearly stoichiometric sorption capacity for CO_2 [12,13]. However, the major challenge is to overcome the loss of sorption capacity during the recarbonation–decomposition cyclic reaction because of the sorbent sintering [14]. It is well known that textural properties of the sorbent drastically affect its recarbonation/decomposition performance under cyclic conditions of the CO_2 capture and biomass gasification [15,16]. To date, several methods have been applied to modify the porous structure of Ca-based sorbents: direct thermal decomposition of natural limestones [17] or Ca-containing salts and hydroxides [18], a wet chemistry route [19], a sol–gel technique [20], hydrolysis of calcium alkoxide precursors, and flame pyrolysis [21]. In all these cases, the porosity and pore size distribution were substantially regulated by the chemical nature of precursors and by synthesis conditions.

On the other hand, textural properties of Ca-based sorbents can be precisely determined via a template approach, in which polymeric microspheres are used as a template [22]. In general, this technique consists of two steps. At the first step, a template, which is formed from microspheres with the definite shape and size, is mixed with the sorbent precursor. At the second step, the precursor is converted to a desired material, while the template is removed by either calcination or extraction [23]. Textural properties of the remained solid replica, such as the macropore size and the specific

* Corresponding author. Boreskov Institute of Catalysis, Pr. Lavrentieva 5, Novosibirsk 630090, Russia.
E-mail address: derevshchikov@mail.ru (V. Derevschikov).

http://dx.doi.org/10.1016/j.micromeso.2016.02.032
1387-1811/

pore volume, are determined by the portion and size of the template. Thus, the template synthesis with nanocasting is a direct technique for the design of materials with appropriate porosity and pore size distribution.

In this work, we used a polystyrene (PS) template to create an additional macroporosity and to design an appropriate pore size distribution in CaO-based sorbents. The effect of the porous structure on the CO_2 sorption performance of the synthesized CaO sorbents during repetitive recarbonation/decomposition cycles was investigated.

2. Experimental

2.1. Sample preparation

The PS templates were synthesized using an emulsifier-free emulsion polymerization technique as described in Ref. [24]. The temperature of the emulsion polymerization was 90 °C. PS spheres with the average sizes of 800 nm or 180 nm were packed by centrifugation at the relative acceleration of 1500. Obtained PS templates were washed with ethanol and dried in air.

CaO was prepared from a micron-sized $CaCO_3$ powder (99% pure, "ReaChim", Russia). The powder was calcined at 900 °C for 3 h in a muffle furnace in air. The product was ground in a mortar. The sorbents were prepared by careful mixing of definite amounts of the CaO powder and the PS spheres with water and ethanol under vigorous stirring with the subsequent grinding in a mortar to prepare a paste suitable for an extrusion molding (Table 1). The required amount of water was determined experimentally using the following criteria: the mixture should be ductile enough to enable extrusion at moderate pressures and hard enough to provide a constant shape of the extrudates. The paste was extruded using a plunger extruder equipped with a 3-mm extrusion die. The extrudates were cut into equal parts, and the obtained pellets were calcined at 900 °C for 3 h in a muffle furnace and then cooled down to room temperature in air.

2.2. Measurements

The alternate recarbonation and decomposition reactions were experimentally studied in a thermogravimetric analyzer Netzsch STA 449 C. About 40 mg of the sample was put in a Pt crucible and heated at the rate of 10 K/min. The recarbonation/decomposition of the sorbents was performed both in a pressure swing adsorption (PSA) mode and in a temperature swing adsorption (TSA) mode. In the PSA mode, both recarbonation and decomposition of the samples were carried out at the same temperature of 740 °C, and the switch between the reactions was provided by switching from the mixture of CO_2 and argon to pure argon (maintaining the same total flow rate). In the case of the TSA mode, the mixture of CO_2 and argon was constantly fed to the analyzer chamber, and the switch between the recarbonation and decomposition was provided by changing the sample temperature from 700 to 1100 °C in a sawtooth manner. In both modes, the experiments were carried out at atmospheric pressure and a total flow rate of 120–150 cm^3/min.

Table 1
Composition of the paste before extrusion.

Sample	CaO, g	PS template, g	Water, ml	Ethanol, ml
CaO-0%	40	0	45	0
CaO-20%PS800 nm	40	10.0	66	0
CaO-40%PS800 nm	20	13.4	37	0
CaO-20%PS180 nm	15	4.0	16	1
CaO-40%PS180 nm	15	10.6	35	4

The flow rates were maintained with two mass flow controllers (RRG-12 type, "ElTochPribor", Russia). Both controllers were preliminary calibrated using a soap film meter, and their stability was routinely checked. The error of setting CO_2 concentration was less than 5%. The dynamic sorption capacity (or total weight change in one cycle) was determined as follows:

$$Weight\ change = \frac{M_{rec} - M_{reg}}{M_o} * 100\%, \quad (1)$$

where M_{rec} is the sample weight at the end of the recarbonation step, M_{reg} is the sample weight at the end of the preceding decomposition step, and M_0 is the weight of the calcined sample.

The sorbents were also characterized using mercury intrusion porosimetry (Micromeritics Autopore VI 2500), low temperature nitrogen adsorption (BET) (Nova 1200e Surface Area and Pore Size Analyzer), scanning electron microscopy (Jeol JSM-6460 LV), and powder X-ray diffraction (Thermo ARL X'TRA). The size of PS template particles was determined by laser diffraction (Mastersizer 2000) and scanning electron microscopy.

3. Results and discussion

3.1. Template particle size determination

We assessed the size of template particles on the basis of the data presented in Fig. 1. The size distribution of the PS particles for both templates was uniform with maximums at 180 and 800 nm, respectively.

3.2. Textural properties of the sorbents

The porous structure of the prepared sorbents was evaluated by the mercury intrusion technique and by the low-temperature nitrogen adsorption (BET) method. Fig. 2 presents cumulative intrusion curves for two series of CaO sorbents obtained from the templates with 180- and 800-nm microspheres. It should be noted that the pore diameter determined from the applied pressure by the Washburn equation refers to the size of the pore mouth. The actual size of macropores is expected to be higher. As seen from Fig. 2, the template approach resulted in a significant increase in the specific pore volume of the CaO sorbent, which was in proportion to the amount of the introduced template. Besides, Fig. 2 clearly demonstrates that the pore volume of the samples synthesized with the addition of 180-nm spheres is higher than the pore volume of the samples with the same amount of the template but with the addition of 800-nm spheres.

Presumably, in the case of the 180-nm template, it was introduced into the composite not in the form of separate spheres but in the form of their aggregates. As a result, inner pores of the aggregates, which were voids unfilled with calcium hydroxide during the synthesis, could contribute to the additional pore volume of these samples.

Fig. 3 shows that for the reference sample (i.e. for the sample synthesized without the template), the maximum of mercury intrusion corresponds to the pore sizes in the range of 100–300 nm. Besides, it is seen that the increase in the amount of the added template leads to a significant shift of the maximum to the higher pore sizes and in a considerable broadening of the distribution peak. These changes in the pore size distribution indicate the sorbent sintering, which was probably a result of local overheating during the template burning.

The local overheating may also be responsible for the higher crystallinity of the templated samples, which was observed by means of the XRD analysis. Indeed, the width of corresponding

Please cite this article in press as: V. Derevschikov, et al., Template technique for synthesis of CaO-based sorbents with designed macroporous structure, Microporous and Mesoporous Materials (2016), http://dx.doi.org/10.1016/j.micromeso.2016.02.032

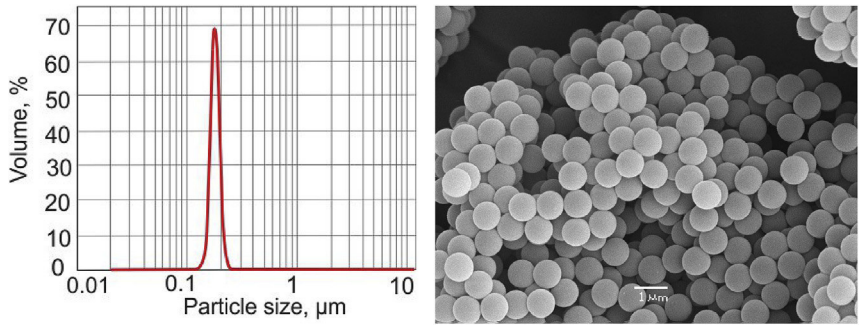

Fig. 1. Laser diffraction data for the 180-nm PS template (a) and electron microscopy image of the 800-nm PS template.

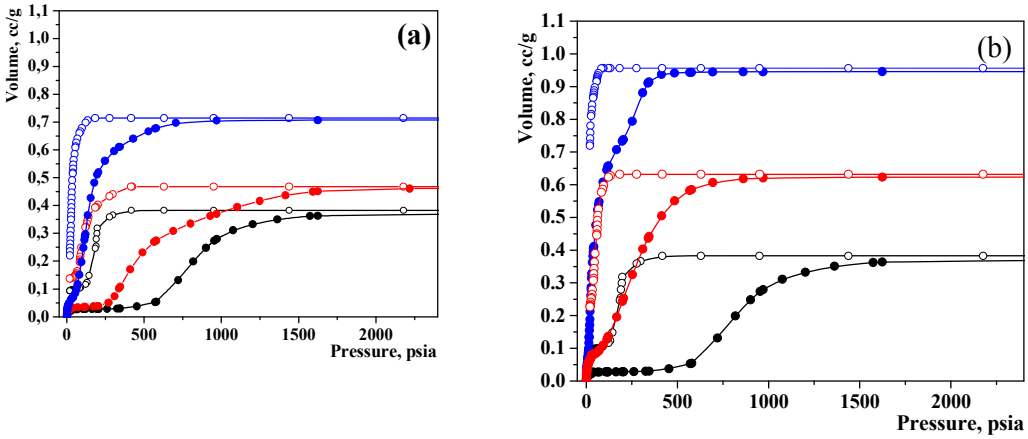

Fig. 2. Mercury intrusion curves for the sorbents prepared using PS templates with two characteristic sizes: 800 nm (a) and 180 nm (b). The data are presented for different portions of the PS template that was introduced to the CaO-PS composite: 0% (black), 20% (red) and 40% (blue). (For interpretation of the references to color in this figure legend, the reader is referred to the web version of this article.)

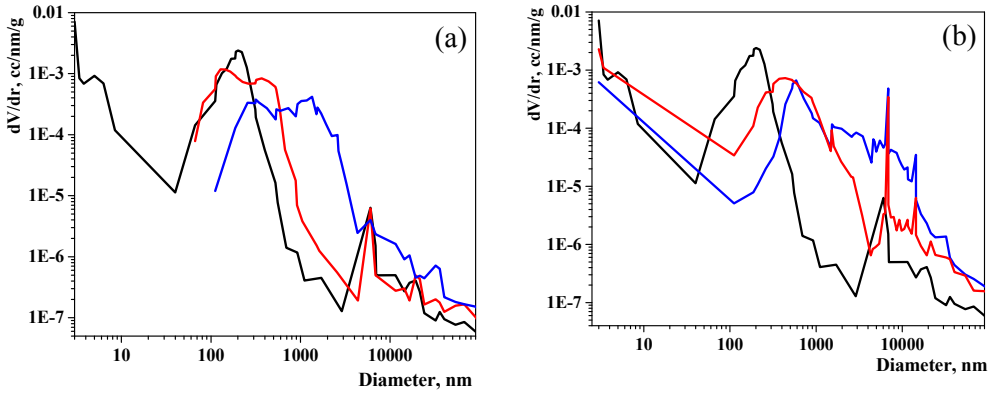

Fig. 3. dV/dr-r plots calculated using mercury intrusion curves for sorbents produced with 800-nm (a) and 180-nm (b) templates. The data are presented for the different portions of the PS template, which were introduced to the CaO-PS composite: 0% (black), 20% (red), and 40% (blue). (For interpretation of the references to color in this figure legend, the reader is referred to the web version of this article.)

diffraction peaks indicates that for the templated samples, the coherent scattering domain (CSD) size started from 170 nm and typically was more than 200 nm, while for the reference sample, the CSD size was about 150 nm (Table 2).

We also compared the data on the pore volume obtained by mercury porosimetry with simple numerical estimates (Table 2). The upper limit for the pore volume of the templated samples can be estimated as the sum of the specific volume of PS and the pore volume of the reference CaO sample:

$$V_{pore\ max} = \frac{\left(\frac{1}{\rho_{PS}} * wt\%_{PS}\right)}{100\%} + V_{Mi}, \quad (2)$$

where $\rho_{ps} = 1.04$ g/cm^3 is the density of PS, and wt%$_{ps}$ is the weight portion of PS. The estimates show that the addition of polystyrene should increase the porosity, but the total pore volume would not exceed 0.57 and 0.77 cm^3/g for the samples with 20% and 40% of the template, respectively. As seen from Table 2, the samples with the 800-nm template met these limits. In contrast, the samples with

Please cite this article in press as: V. Derevschikov, et al., Template technique for synthesis of CaO-based sorbents with designed macroporous structure, Microporous and Mesoporous Materials (2016), http://dx.doi.org/10.1016/j.micromeso.2016.02.032

Table 2
Textural properties of the sorbents.

Sample	Pore volume, cm^3/g (estimated)	Pore volume, cm^3/g (mercury porosimetry)	Porosity (mercury porosimetry)	CSD size, nm	Surface area, m^2/g (mercury porosimetry)	Surface area, m^2/g (BET)
CaO-0%PS	0.38	0.38	0.56	152	13	5
CaO-20% PS800 nm	0.57	0.46	0.61	166	6	3
CaO-40% PS800 nm	0.77	0.71	0.70	>200	3	4
CaO-20% PS180 nm	0.57	0.62	0.67	>200	5	3
CaO-40% PS180 nm	0.77	0.95	0.76	>200	3	1

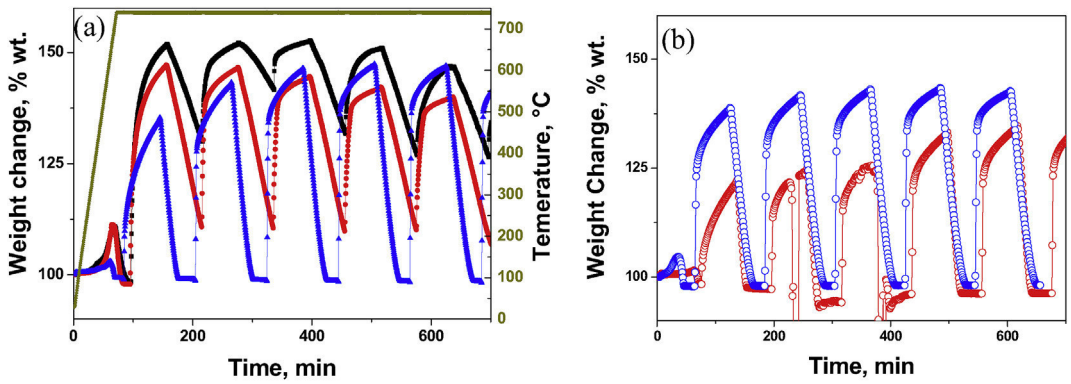

Fig. 4. TG curves during the isothermal segment at 740 °C of the CaO sorbents produced from the composites with 800 nm (a) and 180 nm (b) PS spheres with different portion of the PS template: 0% (black), 20% (red) and 40% (blue). Partial pressure of CO_2 during the sorption step was 33 kPa, gas flow was 100 cm^3/min, total pressure was 101 kPa. (For interpretation of the references to color in this figure legend, the reader is referred to the web version of this article.)

the 180-nm template exhibited the pore volumes that exceeded their estimated limits. As it was supposed above, the extra pore volume could appear because of the inner pores of the PS sphere aggregates, which were inaccessible for calcium hydroxide during the component mixing.

3.3. Sorption properties

Sorption properties of all synthesized samples were measured at 740 °C in the PSA mode. The isothermal segment of the temperature program was long enough to complete approximately six 2-h cycles. All investigated samples showed a significant CO_2 uptake (Fig. 4). At that, during the first recarbonation cycle, the reference sample demonstrated the maximal weight change of 55 wt%, which corresponded to the 70%-conversion of calcium oxide to carbonate. For the PS templated samples, the first-cycle conversion varied from 28% to 64%. The lower recarbonation extent demonstrated by the templated sorbents seems to be caused by the increased size of CaO particles in these samples [25,26] However, in the subsequent cycles, the higher recarbonation extents were observed namely for the templated samples.

To investigate the stability of the sorbents, their dynamic capacity was measured under conditions that are close to the real conditions of the waste gas separation. The dynamic capacity was measured in the TG experiments in the TSA mode. The rate of heating/cooling was 20 K/min, and the partial pressure of CO_2 was 80 kPa during of the whole experiment (Fig. 5).

As seen from Fig. 5, the sorption capacity of the templated sample significantly exceeds the capacity of the reference sample after several cycles. A similar dependence was also observed for lower temperatures, and it most likely seems to be due to the difference in the morphology of the samples.

It is known from the literature that typical depths of the $CaCO_3$ surface layer over the unreacted CaO core change from 50 to 220 nm [27–29] for the wide range of experimental conditions (the sorption times 5–20 min, the temperatures 650–800 °C). Therefore, one should expect that the pores with the diameter less than 220 nm may be completely filled with the carbonate product [25]. In our experiments, this effect led to the smoothing of the external surface of the sorbents and to reducing their surface area after the

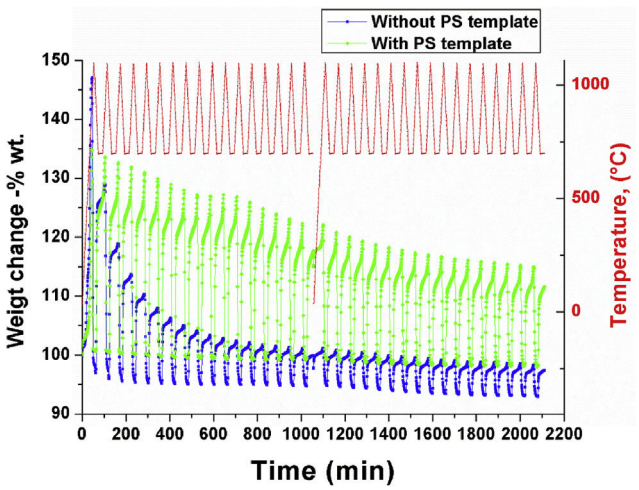

Fig. 5. TG curves of the CaO sorbents prepared without a template (blue) and with the 800-nm PS template (the portion of the template was 40%) (green). The partial CO_2 pressure during the experiment was 80 kPa, the gas flow was 100 cm^3/min, and the total pressure was 101 kPa. (For interpretation of the references to color in this figure legend, the reader is referred to the web version of this article.)

Please cite this article in press as: V. Derevschikov, et al., Template technique for synthesis of CaO-based sorbents with designed macroporous structure, Microporous and Mesoporous Materials (2016), http://dx.doi.org/10.1016/j.micromeso.2016.02.032

recarbonation step (Fig. 6). Indeed, the SEM images show that pores of the reference sample are almost totally filled with the product, while a part of large transport macropores remain free in the templated sorbent after a series of the recarbonation/decomposition cycles (Fig. 6).

The apparent difference in the pore structure resulted in the striking difference in the decomposition rates of the sorbents (Fig. 7). While the decomposition of the reference sample and CaO-20% PS800 nm did not complete in 60 min, the other samples totally decomposed during the decomposition step. The average decomposition rate for the reference sample was about 0.3 wt %/min for the first 30 min, while the highly porous templated samples showed an order of magnitude higher decomposition rates. The highest rate of 3.0 wt%/min was observed for CaO-40% 180 nm.

It has been shown in Ref. [30] that at low CO_2 pressures, the decomposition rate quickly decreases with an increase in the particle size. This indicates that the reaction is limited by CO_2 transportation inside pores from the external particle surface. However, an increase in the partial pressure of CO_2 during decomposition results in a very rapid decrease in the decomposition rate. At relatively high partial pressures of CO_2, i.e. at pressures close to the equilibrium pressure over $CaCO_3$, the rate becomes insensitive to the particle size, indicating that decomposition becomes reaction-rate-limited rather than diffusion-limited [30]. Taking into account that the pellets used in our experiments and the pellets used in Ref. [30] were of a similar size, we may assume that the internal pellet porosity accelerates the decomposition. It seems that higher porosity provides better drainage of carbon dioxide from the core to the external surface of a pellet, more effectively decreases the partial pressure of CO_2 on the $CaO/CaCO_3$ surface and thereby increases the decomposition rate.

In a porous solid with interconnected pathways, a gas molecule may collide with another molecule or with pore walls. When the gas pressure is high, molecule–molecule collisions dominate, which situation is referred to as the Fickian regime. At the small pore size, collisions between molecules and pore walls dominate, which is called the Knudsen diffusion regime. When both mechanisms are of importance, the combined diffusion coefficient D may be written as a combination of the Fick (D_{Fick}) and Knudsen (D_{Knud}) diffusion coefficients [31]:

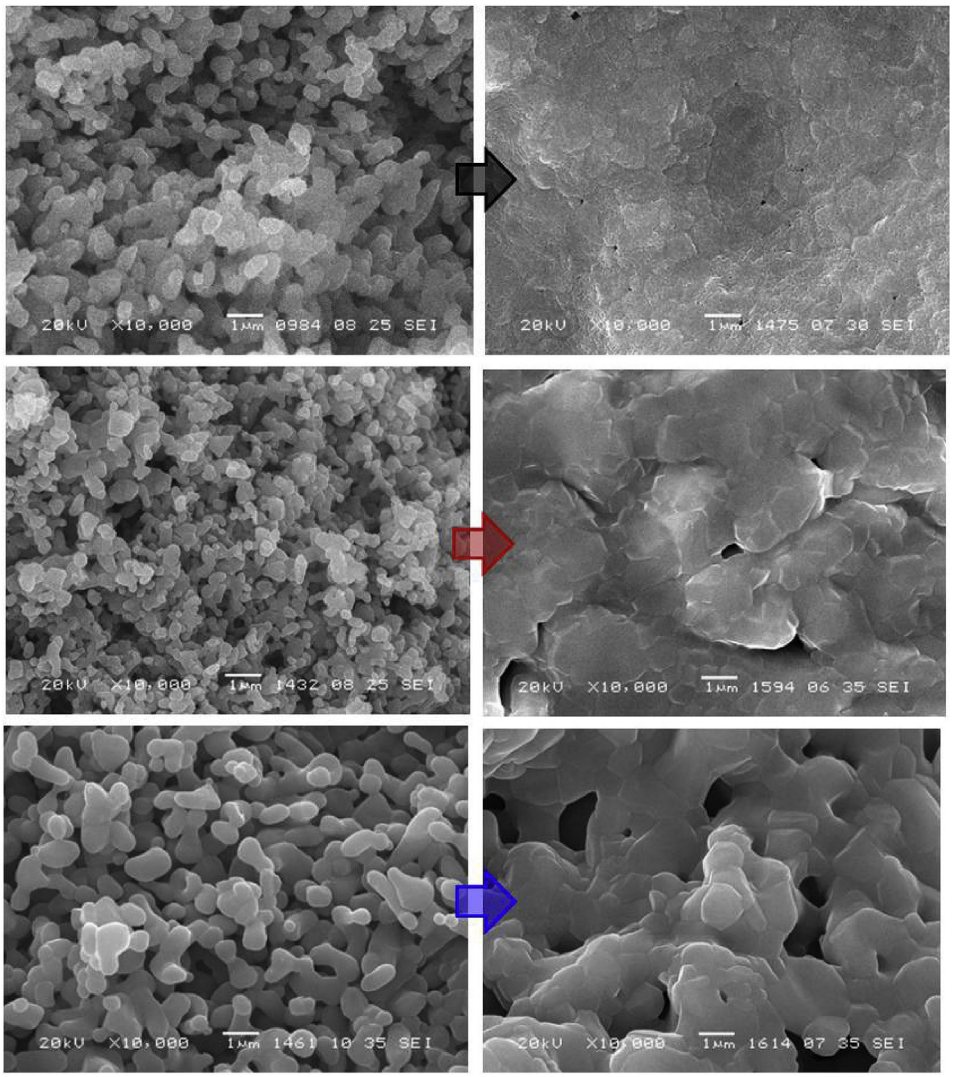

Fig. 6. SEM images of the fresh sorbents (left) and sorbents after several cycles and after 1-h recarbonation at 740 °C (right) with different portion of the 800-nm PS template: 0% (top panels), 20% (middle panels) and 40% (bottom panels). The partial pressure of CO_2 during the sorption step was 33 kPa, the gas flow was 100 cm^3/min, and the total pressure was 101 kPa.

Please cite this article in press as: V. Derevschikov, et al., Template technique for synthesis of CaO-based sorbents with designed macroporous structure, Microporous and Mesoporous Materials (2016), http://dx.doi.org/10.1016/j.micromeso.2016.02.032

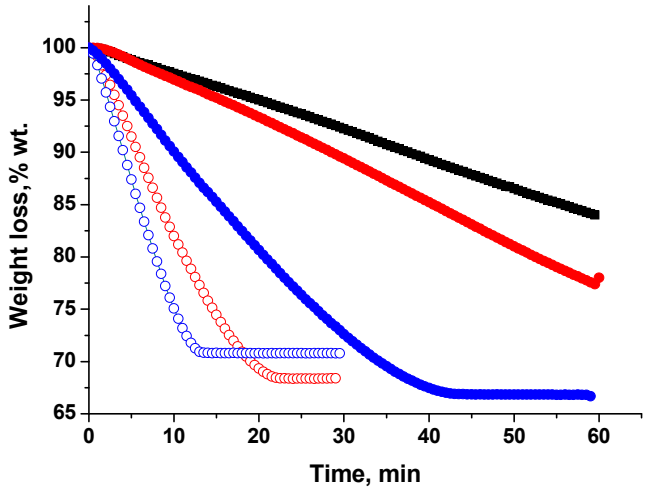

Fig. 7. Decomposition rates of different sorbents during the 4th cycle. The samples were produced from the composites with 800 nm (solid symbols) and 180 nm (open symbols) PS spheres with different portions of the PS template: 0% (black), 20% (red), and 40% (blue). (For interpretation of the references to color in this figure legend, the reader is referred to the web version of this article.)

$$\frac{1}{D} = \frac{1}{D_{Knud}} + \frac{1}{D_{Fick}} = 3 \cdot \left(\frac{1}{d_{pore}\bar{u}_1} + \frac{1}{\lambda \bar{u}_{12}} \right), \tag{3}$$

where $\bar{u}_1$ is the mean velocity of CO_2 molecules, $\bar{u}_{12}$ is the mean velocity of CO_2 molecules relative to the inert gas, d_{pore} is a typical pore diameter, and λ is the mean free path. It follows from Eq. (2) that in solids with small pores, the Knudsen diffusion is limiting. Fig. 6 shows that after the recarbonation step, the templated samples have much larger pores than the reference sample does. These pores facilitate the CO_2 transport out of the grain during the subsequent decomposition step.

The high pore volume may also contribute to the higher decomposition rate. The sample porosity ϕ and tortuosity τ of the pores affect the effective diffusion coefficient D_{eff} according to the formula [31]:

$$D_{eff} = D\frac{\phi}{\tau} \tag{4}$$

After decomposition, the templated samples have the pore volume that is up to 2.5 times higher than that of the reference sorbent (Table 2). The ratio of the pore volumes in the recarbonated samples is even more in favor of the templated samples. According to the skeleton model [25], the total volume of the sorbent grain does not change after the skeleton formation. Using this assumption, one can estimate the pore volume $V_{\text{pore,rec}}$ after the recarbonation step from the pore volume $V_{\text{pore,CaO}}$ of the decomposed sorbent:

$$\begin{aligned} V_{pore,CaO} + \frac{1}{\rho_{CaO}} &= V_{pore,rec} + \frac{C_{PB} \cdot x_r + (1 - x_r)}{\rho_{CaO}} \\ V_{pore,rec} &= V_{pore,CaO} - \frac{(C_{PB} - 1) \cdot x_r}{\rho_{CaO}} \end{aligned} \tag{5}$$

where $\rho_{CaO} = 3.35 \frac{g}{cm^3}$ is the CaO bulk density, $C_{PB} = 2.2$ is the Pilling–Bedworth ratio (molar volume ratio) for $CaCO_3$ and CaO, and x_r is the recarbonation extent. Both templated and reference sorbents demonstrate similar recarbonation extents of about 60%. Estimation by formula (5) yields $V_{\text{pore,rec}}$ of 0.17 cm^3/g and 0.74 cm^3/g for the reference sample and for CaO-40%PS180 nm, respectively. Thus, after the recarbonation step, the pore volume ratio for these samples jumps to 4.5, which explains almost half of the observed decomposition rate effect.

4. Conclusions

It has been shown that the template approach can be used as a direct and apparent method for the formation of a porous structure of CaO-based sorbents. The porosity that appeared in the sorbent after the template burning is not equal to the initial volume of the template and depends on the size and the amount of the template. The recarbonation-decomposition properties of the synthesized sorbents clearly demonstrate that the more developed porous structure provides high rates of the carbon dioxide release, which is crucial for practical applications. It has been also shown that the dynamic sorption of the sorbents prepared with the template is higher than the capacity of the sorbents prepared in the absence of the template. Therefore, we suppose that the template synthesis technique will be a perspective way to enhance the sorption capacity of CaO-based sorbents.

Acknowledgments

The authors are grateful to Dr. A.A. Sidelnikov for productive discussion. The work was performed in the framework of the joint Research and Educational Center for Energy Efficient Catalysis (Novosibirsk State University, Boreskov Institute of Catalysis) under partial support of RFBR (Research project No. 16-33-00436 mol_a).

References

[1] J. Wang, V. Manovic, Y. Wu, E.J. Anthony, Chem. Eng. Trans. 21 (2010) 643–648.
[2] V. Nikulshina, a. Steinfeld, Chem. Eng. J. 155 (2009) 867–873.
[3] H.K. Park, M.W. Bae, O.S. Yoon, S.G. Kim, Chem. Eng. J. 195–196 (2012) 158–164.
[4] F.N. Ridha, V. Manovic, Y. Wu, A. Macchi, E.J. Anthony, Int. J. Greenh. Gas. Control 16 (2013) 21–28.
[5] J. Mastin, A. Aranda, J. Meyer, Energy Procedia 4 (2011) 1184–1191.
[6] N.H. Florin, A.T. Harris, Chem. Eng. Sci. 63 (2008) 287–316.
[7] N.H. Florin, A.T. Harris, Energy Fuels 22 (2008) 2734–2742.
[8] J. Blamey, E.J. Anthony, J. Wang, P.S. Fennell, Prog. Energy Combust. Sci. 36 (2010) 260–279.
[9] M. Alonso, N. Rodríguez, B. González, G. Grasa, R. Murillo, J.C. Abanades, Int. J. Greenh. Gas. Control 4 (2010) 167–173.
[10] J.C. Abanades, E.J. Anthony, J. Wang, J.E. Oakey, Environ. Sci. Technol. 39 (2005) 2861–2866.
[11] S.S. Kazi, A. Aranda, J. Meyer, J. Mastin, Energy Procedia 63 (2014) 2207–2215.
[12] M. V Iyer, H. Gupta, B.B. Sakadjian, L.S. Fan, Ind. Eng. Chem. Res. 43 (2004) 3939–3947.
[13] H. Lu, P.G. Smirniotis, F.O. Ernst, S.E. Pratsinis, Chem. Eng. Sci. 64 (2009) 1936–1943.
[14] S.D. Angeli, C.S. Martavaltzi, A. a. Lemonidou, Fuel 127 (2014) 62–69.
[15] D.T. Beruto, A.W. Searcy, M.G. Kim, Thermochim. Acta 424 (2004) 99–109.
[16] F. García-Labiano, a. Abad, L.F. de Diego, P. Gayán, J. Adánez, Chem. Eng. Sci. 57 (2002) 2381–2393.
[17] B.R. Stanmore, P. Gilot, Fuel Process. Technol. 86 (2005) 1707–1743.
[18] K.O. Albrecht, K.S. Wagenbach, J.A. Satrio, B.H. Shanks, T.D. Wheelock, Ind. Eng. Chem. Res. 47 (2008) 7841–7848.
[19] C. Luo, Y. Zheng, Y. Xu, N. Ding, Q. Shen, C. Zheng, Chem. Eng. J. 267 (2015) 111–116.
[20] M. Broda, C.R. Müller, Fuel 127 (2014) 94–100.
[21] L. Hong, A. Khan, S.E. Pratsinis, P.G. Smirniotis, Energy Fuels 23 (2009) 1093–1100.
[22] B.T. Holland, C.F. Blanford, A. Stein, Sci. (80-.) 281 (1998) 538–540.
[23] O. Sel, D. Kuang, M. Thommes, B. Smarsly, Langmuir 22 (2006) 2311–2322.
[24] K.A. Sashkina, V.S. Labko, N. a. Rudina, V.N. Parmon, E.V. Parkhomchuk, J. Catal. 299 (2013) 44–52.
[25] A.I. Lysikov, A.N. Salanov, A.G. Okunev, Ind. Eng. Chem. Res. 46 (2007) 4633–4638.
[26] P. Lan, S. Wu, Fuel 143 (2015) 9–15.
[27] A.G. Okunev, a. I. Lysikov, Russ. J. Appl. Chem. 84 (2011) 173–178.
[28] J.C. Abanades, D. Alvarez, Energy Fuels 17 (2003) 308–315.
[29] D. Alvarez, J.C. Abanades, Energy Fuels 19 (2005) 270–278.
[30] A.G. Okunev, S.S. Nesterenko, a. I. Lysikov, Energy Fuels 22 (2008) 1911–1916.
[31] G.K. Boreskov, Heterogeneous Catalysis, 1986. Nauka, Moscow.

Please cite this article in press as: V. Derevschikov, et al., Template technique for synthesis of CaO-based sorbents with designed macroporous structure, Microporous and Mesoporous Materials (2016), http://dx.doi.org/10.1016/j.micromeso.2016.02.032

Evolution of Textural Properties of CaO-based Sorbents during Repetitive Sorption/Regeneration Cycles

Ya.V. Bazaikin †‡ ♭ , E.G. Malkovich †‡, V.S. Derevschikov †§, A.I Lysikov †§ and A. G. Okunev †§

† Novosibirsk State University, pr.Koptyuga 1, Novosibirsk 630090, Russia

‡Sobolev Institute of Mathematics, pr.Koptyuga 4, Novosibirsk 630090, Russia

§ Boreskov Institute of Catalysis, pr.Lavrentieva 5, Novosibirsk 630090, Russia

♭ Faculty of Science, University of Hradec Kralove, Rokitanskeho 62, Hradec Kralove 50003, Czech Republic

ABSTRACT

The evolution of sorptive and textural properties of CaO-based sorbents during repetitive sorption/regeneration cycles has been mathematically modeled. The proposed model takes into account the morphology of nascent CaO, sorbent sintering, and carbonation kinetics. The results show that the model is in good agreement with experimental data for real sorbents and predicts well the dependence of the recarbonation extent on the number and duration of the sorption/regeneration cycles.

1. INTRODUCTION

Emission of large amounts of CO_2 to the atmosphere, mostly as a by-product of burning fossil fuels, sufficiently contributes to the climate change [1,2]. The need to move toward a sustainable energy future motivates the search for new technologies to meet the ever-growing world energy demand. One of the options for reducing greenhouse gas emissions is the CO_2 capture and storage from large stationary sources[3] and during biomass gasification by means of solid sorbents[4]. Some studies on this topic suggest the use of calcium-based sorbents for the effective capture of CO_2 at high temperatures based on the reversibility of the reaction [5]:

$$CaO+CO_2 \rightleftarrows CaCO_3.$$

From a cost point-of-view, limestone should have a fairly obvious advantage [8]. However, the use of natural calcium carbonates as regenerable sorbents of CO_2 is limited by the rapid decay of the carbonation conversion with the number of carbonation/calcination cycles [9]. Alvarez and Abanades [10] have shown that the recarbonation is far from being reversible in practice and the main reasons for the CaO capacity decay are the sorbent sintering and pore blockage.

In order to describe the CaO capacity decay during repetitive sorption/regeneration cycles, a number of semi-empirical equations have been proposed. Wang and Anthony[11] derived an

expression similar to that used for catalyst deactivation through sintering. They suggested that the carbonation extent X_N is inversely proportional to the number *N* of cycles and tends to zero.

$$X_N = \frac{1}{1+kN} \quad (1)$$

where *k* is constant characterized the intensity of the sintering in cycles.

Grasa and Abanades[12] modified this equation with X_∞ —the recarbonation extent after an infinite number of cycles — to account for the residual CaO capacity in a long series of recarbonation-decomposition cycles:

$$X_N = \frac{1}{\frac{1}{1-X_\infty} + kN} + X_\infty \quad (2)$$

Lysikov and Okunev[13] reported that the addition of the sintering exponent n ($\approx$ 0.58) significantly improves the agreement of the equation with experimental data.

$$X_N = \frac{1-X_\infty}{(1+kN)^n} + X_\infty \quad (3)$$

Although the proposed equations are in reasonable agreement with practice, it is important to take into account the role of textural characteristics of the sorbents (e.g., the surface area and pore size) for a more detailed modeling and prediction of the sorbent performance [14].

Qualitatively the mechanism of textural transformations of CaO that may take place in the cycling environment was described in [13] as follows (Figure 1). First, decomposition of original $CaCO_3$ leads to the formation of smaller particles of CaO. Further, the freshly calcined sorbent recarbonates incompletely because of the shrinking of the particles during the first decomposition. In the following cycles, newly formed CaO grains grow and agglomerate. The necks between adjacent CaO grains thicken and strengthen until they can withstand the recarbonation stage. At the final step, the network of the interconnected CaO particles (a so-called skeleton) is formed and ceases the subsequent sintering. After that, only the outer layer of the skeleton recarbonates, while its internal CaO core is protected by the product $CaCO_3$ layer and may be considered as a refractory support for the outer reactive CaO shell.

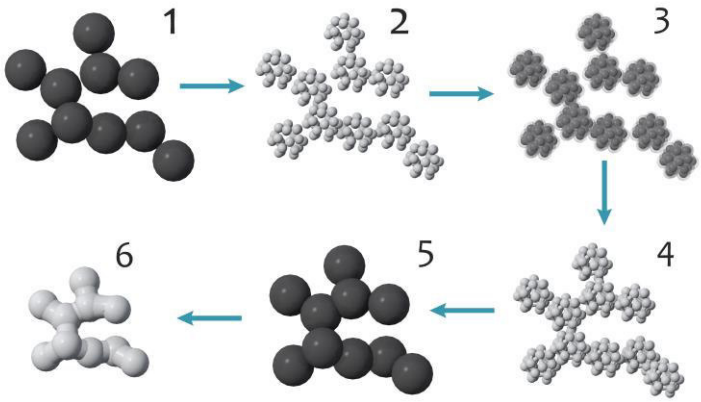

Figure 1. Scheme of sorbent textural transformations. Reprinted (adapted), with permission, from Ref. [13]. Copyright 2007, American Chemical Society.

Bridging the gap between the qualitative and quantitative descriptions of the CaO sintering mechanism seems to be an important step on the way to predict the behavior of some important sorbent characteristics (such as sorption capacity, surface area, and pore distribution) during a sorption/regeneration process.

Sun et al. in [15,] described the decay mechanism in terms of the sintering kinetics[16] as a decrease in the surface area and pore volume

$$\left(\frac{dS}{dt}\right)_{sintering} = k_s(S - S_a)^2 \quad (4)$$

where S is present surface area, S_a is original surface area, and k_s is sintering constant.

Another method to characterize porous materials is based on topological algorithms[17]. This method allows one to take into account the real geometric structure of porous materials and thus to model their properties and processes[18] (e.g., fluid transport, deformation, and sintering) on a higher level of accuracy.

The present study had two objectives: first, using the novel topological approach in combination with the sintering concept, to design a reliable model for the deactivation of CaO-based sorbents; and second, to use this model to explore how reaction parameters (cycle duration, rates of carbonation/decomposition reactions) and the porous structure of parent CaO affect the sorption performance of CaO in recarbonation-decomposition cycles.

2. METHODS

Modeling for the carbonation/decomposition process of the CaO granule using its textural characteristics.

Granule sintering model.

In the current study, we used experimental data of Lysikov et al. on the synthesis of monodisperse (3.5-4.5 μm) calcium carbonate [19] and on the sorption properties of the derivate sorbent [13] as reference data for the model. It should be noted that the first decomposition of initial monodisperse calcium carbonate leads to the formation of smaller, partially connected grains of CaO (Figure 2).

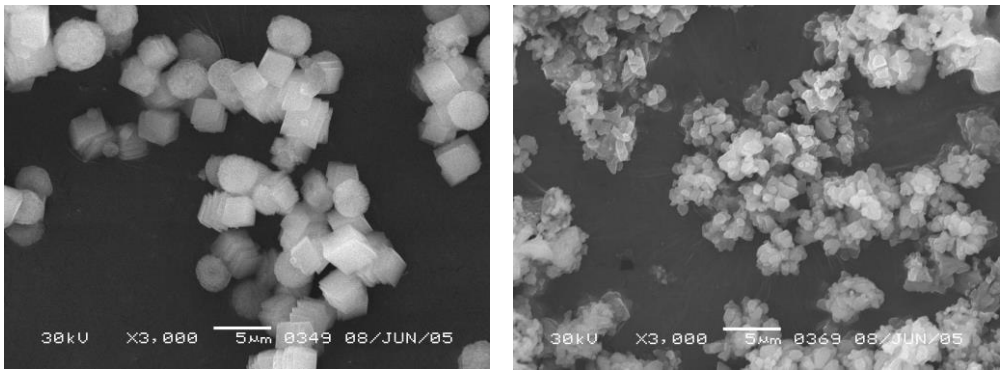

Figure 2. SEM images of parent $CaCO_3$ (left) and derived CaO (right) after 2-hour calcination at 1100°C.

As clearly seen from Figure 2, the surface of formed calcium oxide represents a sintered compact of sphere-like particles with necks between them. Therefore, a granule in our model was simulated with the dense random packing of N spheres of the same radius in a cube with the edge L using the Lubachevsky-Stillinger (LS) compression algorithm [20]. Work time of the LS algorithm can be managed by the packing density $\rho = V_s/V_c$, where V_s and V_c are volumes of the grains and the cube, respectively. For large values of N, one can assume that

$$\rho = \frac{4\pi}{3}\frac{R^3}{L^3} \tag{5}$$

where R is a sphere radius. However, this formula is not exact because of the grains supported along the walls of the cube (we call it the *wall-effect*). Therefore, we used a more precise variant:

$$\rho = \frac{\sum_{i=1}^{N}\sum V_i^{int}}{(L-2R)^3} \tag{6}$$

where V_i^{int} is the volume of the intersection of an i-th grain and a cube with the edge $L - 2R$ and with the same center as the initial cube. Porosity ε is one of the main characteristics of porous media, and for the dense sphere packing, it can be estimated as $\varepsilon = 1 - \rho$.

It is well known that the maximum density of the sphere packing is ≈ 0.74 and it is achieved on the face-centered cubic lattice. This statement is equivalent to the Kepler conjecture and now is widely considered proven by T.C. Hales. Random packings can have different densities, but usually porosity of the media simulated by random sphere packings maintains values $0.38 \pm$

0.02. The porosity of CaO granules found by the mercury porosimetry is $\varepsilon_{por} = 0.38\ mL/g$, the real density of CaO is $p = 3.34\ g/mL$, so the non-dimensional porosity of CaO is

$$\varepsilon = \frac{\varepsilon_{por}}{1/p+\varepsilon_{por}} \approx 0.559\,. \quad (7)$$

An early stop of the LS algorithm can provide an appropriate porosity ε, but it gives a too small number of sphere contact points in the packing. Therefore, we proceeded as follows:

1) We modeled sufficiently dense random packing with porosity ≈ 0.4 using the LS-algorithm.

2) We "threw out" a part of the grains to maintain the needed porosity.

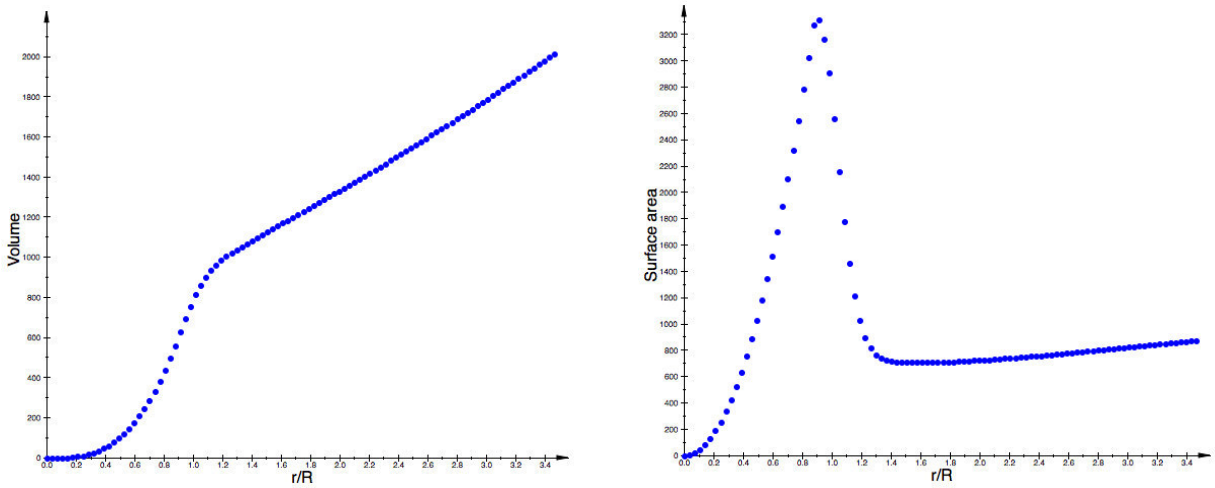

Figure 3. Volume (left) and free surface (right) of the set of spheres with radius r. Vertical lines correspond to $r = R$, i.e. to the radius of spheres in the dense packing.

Let the sphere centers form the set $\mathcal{P} = \{\bar{u}_i, i = 1, \dots, N\}, 0 \le \bar{u}_i \le L$, the radius of each sphere is R. Denote as $V(r)$ the total volume of the spheres with centers in $\mathcal{P}$ and with radius r. The function $V(r)$ is shown in Fig. 3. We can see that the tangent of $V(r)$ decreases after $r > R$, i.e. after the moment when the spheres begin to intersect. Almost at the same moment, the free surface begins to decrease. We suppose that in the sorption-regeneration cycle, the layer of $CaCO_3$ grows from the surface of the grain in two directions —outside and inside the grain — with thickness d each. Then, the volume of $CaCO_3$ formed during the sorption stage is calculated by

$$\delta V = V(R + d) - V(R - d) \quad (8)$$

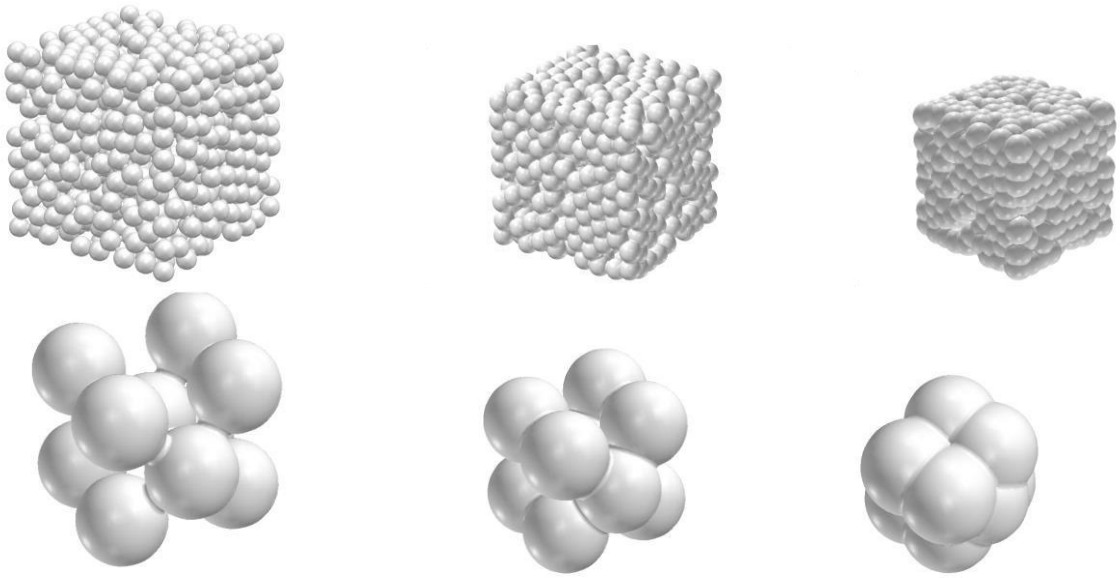

Figure 4. Different stages of sintering: $\mu = 1$ (initial example, left); $\mu = 0.8$ (center); $\mu = 0.5$ (right). Below: typical sectors of the appropriate examples.

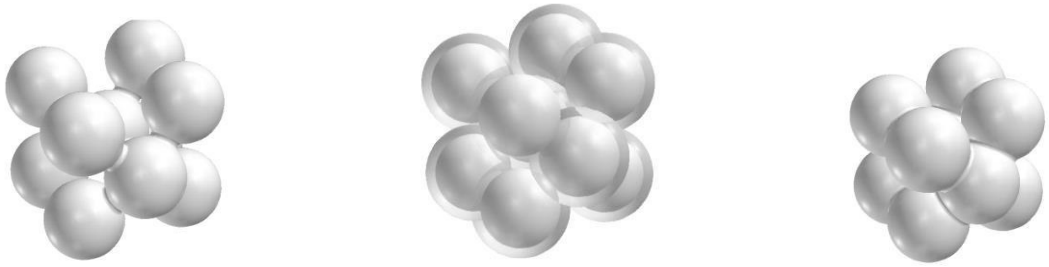

Figure 5. Sorption/regeneration stages of the grains sintering.

We suppose that the sintering of the CaO granule at high temperature causes an approach of grain centers and a decrease in the linear size of the granule from L to μL. The coefficient μ here is the *shrinkage* factor, and this is the main parameter of sintering in our model. Fig. 4 demonstrates the stages of sintering for the different coefficients μ. Fig. 5 depicts the stage of forming the layer of $CaCO_3$ with the subsequent sintering. Thus, we have an initial set of sphere centers $\mathcal{P} = \mathcal{P}_1$ and the volume function $V(r)$. After the sintering, we will have the packing with centers $\mathcal{P}_\mu = \{\mu\bar{u}_i, i = 1, \dots, N\}$ and with the same radii R. Let us denote the volume of the spheres with radii r and with centers $\mathcal{P}_\mu$ as $V_\mu(r)$. It is easy to check that

$$V_\mu(r) = \mu^3 V\left(r/\mu\right) \quad (9)$$

The volume of $CaCO_3$ formed in one sorption/regeneration cycle for the sintered granule is

$$\delta V_\mu = \mu^3 V\left(\frac{R+d}{\mu}\right) - \mu^3 V\left(\frac{R-d}{\mu}\right) \quad (10)$$

If the initial volume of CaO in the granule is V_0, then the initial amount of CaO is

$$\nu_0 = V_0 \frac{\rho_{CaO}}{M_{CaO}} \quad (11)$$

where ρ_{CaO} is real density of CaO and M_{CaO} is its molar mass. If in a certain cycle, the sorption of CO_2 resulted in the formation of a volume δV_μ of $CaCO_3$, then the amount of CaO reacted in that cycle is

$$\nu = V_\mu \frac{\rho_{\mathrm{CaCO3}}}{M_{\mathrm{CaCO3}}} \quad (12)$$

Consequently, the recarbonation extent is

$$RE = \Lambda \frac{\mu^3 \left(V\left(\frac{R+d}{\mu}\right) - V\left(\frac{R-d}{\mu}\right)\right)}{V_0} \quad (13)$$

where

$$\Lambda = \frac{\rho_{\mathrm{CaCO3}}}{\rho_{CaO}} \frac{M_{CaO}}{M_{\mathrm{CaCO3}}} \approx 0.46 \quad (14)$$

2. Dynamics of the shrinkage factor μ in a repetitive sorption/regeneration process.

The layer of $CaCO_3$ is growing while CaO reacts with CO_2. We suppose that for a time t, the layer of $CaCO_3$ grows in thickness $d = d(t)$ inside and outside of each grain and can be described as a spherical layer $R - d \leq r \leq R + d$. During the adsorption, the thickness of the carbonate layer increases. This hinders the diffusion of CO_2 through it, which in turn decelerates the formation of the carbonate layer. Numerous works have been made to determine the kinetics of CaO carbonation and to determine the rate of carbonate layer formation [21]. In this work, we consider the following time dependence of the layer formation:

$$d(t)^n = D^n t \quad (15)$$

where D is the diffusion coefficient. [24]

Such dependence is typical of the reaction of solid with gas [22] and is valid when the partial pressure of CO_2 repeatedly exceeds the equilibrium [23].

The sintering that takes place during the cycling and that changes the texture of the original sorbent seems to occur by both lattice and surface diffusion mechanisms [15].

The lattice diffusion mechanism of the sintering is characterized by the shrinkage, i.e. by reduction of the distance between the centers of sintered particles. In contrast, the surface diffusion mechanism does not lead to the shrinkage[25].

During the shrinkage, the healing of small pores and the growth of large pores occur. As a result, the average pore size increases and the total pore volume decreases. Because a similar behavior was confirmed experimentally [26], in the current study, we used an assumption wherein the

decrease in the sorbent recarbonation extent from cycle to cycle occurs only because of the shrinkage.

Previously, Borgwardt [27,28] has shown that the rate of a decrease in the CaO surface area (i.e. the rate of sintering) significantly increases in the CO_2-containing atmosphere even at the temperatures above equilibrium for $CaCO_3$ formation. He explained this phenomenon with the change in the sintering mechanism to a faster surface-like diffusion that is catalyzed by carbon dioxide. In many later works (Grasa, Lysikov), it was shown that the sintering on the sorption step proceeds much more intensely than it does on the regeneration step at the same temperature. The strong difference in the Tamman temperatures for carbonate and oxide indirectly confirms the higher mobility of ions in the $CaCO_3$ crystal lattice compared with that in CaO, thus the mass transfer rate in carbonate is faster than that in oxide under the same conditions.

The grains begin to sinter during the sorption because the growing layer of $CaCO_3$ has high mobility. First, we consider a pair of grains in the sorption process as intersected spheres of radii R with the distance between their centers $2l \leq 2R$ (Fig.6). The contact area between the spheres is a circle of radius x, where $x^2 = R^2 - l^2$ (Fig.6). We will ignore the deformation of the grains during the sorption. Unreacted CaO fills the spheres with radii $R - d$ and with the same centers. $CaCO_3$, which appeared in the sorption process, forms the layer of the thickness $2d$. The sorption proceeds at the temperatures 750-850°C, which provides the mobility of the $CaCO_3$ layer but prevents the sintering of unreacted CaO.

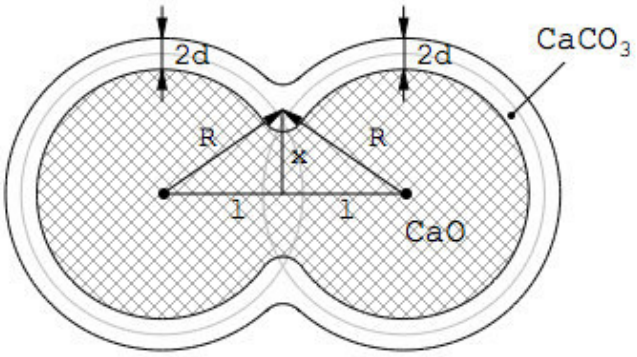

Figure 6. Sintering of two grains.

Because of its mobility, the layer of $CaCO_3$ tends to decrease in volume. The energy of the system is consumed for a decreasing of the distance between the centers (there appears a force F that squeezes the grains to each other) and for a resistance of non-reacted CaO grains to smash each other. If the force F does not produce a pressure greater than the ultimate tensile strength, then the centers do not approach. After achieving the critical thickness of the layer, the plasticity

in the contact zone appears and the grains begin to get closer. We will suppose that the force F is proportional to the surface tension ($\sim R$) and the layer thickness ($\sim d$). Thus,

$$F = \alpha R d \ (16)$$

where coefficient α is the specific volume energy of the $CaCO_3$ layer.

In the contact zone, the force F generates the normal tension equal to

$$\sigma = \frac{F}{\pi(x-d)^2} \ (17)$$

Centers begin to approach, if

$$\sigma \geq \sigma_0, F \geq F_f = \sigma_0(x-d)^2 \ (18),$$

where σ_0 and F_f are the critical values of tension and force respectively after achieving that the coalescence of particles begins.

In the following process of grain approaching, the force is equal to $F - F_f \geq 0$, and the motion of CaO is described by the Newton's second law.

$$m\frac{d^2l}{dt^2} = -\left(F - F_f\right) = -\alpha R d(t) + \pi\sigma_0(x-d)^2 (19)$$

where m is the mass of unreacted CaO in one grain. We will suppose also that d is small with respect to R and x. By setting $\kappa^2 = \pi\sigma_0/m\,, \omega^2 = \alpha/(\pi\sigma_0),$ we get

$$\frac{d^2l}{dt^2} = -\kappa^2(\omega^2 R d(t) - R^2 + l^2) \ \ (20)$$

The assumption of smallness of d breaks in the very first moment of sintering when x is small (or even vanishes) and the force F_f does not act because CaO grains do not touch each other. In this case, equation (19) still holds.

Let us consider the sequence of sorption/regeneration cycles with the sorption duration equal to T. The initial distance between grain centers is $2l_0 = 2R. (21)$

Every next cycle will provide the grain approach starting at the moment when $F \geq F_f$ and until the thickness of the $CaCO_3$ layer becomes $d_T = d(T) = DT^{\frac{1}{n}}. (22)$ The critical distance between centers is $2l_\infty$ for a given T and can be defined from the following identity

$$l_\infty^2 = R^2 - \omega^2 R d_T = \ R^2 - \omega^2 R D T^{\frac{1}{n}} \ (23)$$

Consider a k-th cycle, in the beginning of which the distance between centers equals $2l_k$. The approach of the centers starts if $F = F_f$, so we can calculate the time t_k when the movement begins:

$$t_k = \left(\frac{R^2 - l_k^2}{\omega^2 R D}\right)^n \ (24)$$

The sequence l_k can be found from the following iterating sequence of Cauchy problems:

$$l_0 = R \quad (25)$$

$$t_k = \left(\frac{R^2 - l_k^2}{\omega^2 RD}\right)^n \quad (26)$$

$$\frac{d^2 l}{dt^2} = -\kappa^2(\omega^2 R d(t) - R^2 + l^2) \quad (27)$$

$$l(t_k) = l_k, \frac{dl}{dt}(t_k) = 0 \quad (28)$$

$$l_{k+1} = l(T) \quad (29)$$

Note that $l_k \to l_\infty$ if $k \to \infty$. In addition, we observe that the mass m can be considered as depending on time t weakly for $t_k \le t \le T$ and in system (2) we can put κ as a constant. Nevertheless, as T changes, the coefficient κ can change greatly, and actually $\kappa = \kappa(T)$ (30)

If we consider the whole granule, we can assume that it shrinks only because of the approaching of all pairs of contacting grains (we ignore small distortions of the granule), and the shrinkage factor after the k-th cycle can be calculated as

$$\mu_k = \frac{l_k}{R} \quad (31)$$

Let us denote the non-dimensional parameter $\delta(t) = d(t)/R$, which is such a part of a grain layer that reacts during the sorption. The parameter $\mu_\infty = l_\infty/R$ is a limit shrinkage factor of the sample. $\delta_T = \delta(T)$ 32) is a part of maximal thickness of the $CaCO_3$ layer with respect to grain radius at predetermined T. We use the following iterative equations that allow one to average the dynamics of μ_k:

$$\mu_0 = 1 \quad (33)$$

$$\mu_\infty = \sqrt{1 - \omega^2 \delta_T} \quad (34)$$

$$\mu_{k+1} = \mu_k - \kappa^2 T^2 (\mu_k^2 - \mu_\infty^2)\left(1 - \left(\frac{1 - \mu_k^2}{1 - \mu_\infty^2}\right)^n\right)^2 \quad (35)$$

Equation 35 allows one to estimate the recarbonation extent after the k-th cycle:

$$RE_k = \Lambda \frac{\mu_k^3 \left(V\left(\frac{1 + \delta_T}{\mu_k} R\right) - V\left(\frac{1 - \delta_T}{\mu_k} R\right)\right)}{V_0} \quad (36)$$

Putting $\mu_k = \mu_\infty$, we obtain the stationary limit recarbonation extent of the CaO granule[25,29].

3. RESULTS AND DISCUSSIOINS

Numerical experiment and real experiment.

The first two experiments show the dependence of the recarbonation extent (RE) on two parameters: duration T of the carbonation stage (which influences the thickness d of the $CaCO_3$ layer) and the limit shrinkage factor μ. Smaller values of μ force smaller free surface areas of the grain surface and smaller REs but may be compensated by longer carbonation duration, and vice versa.

In the first experiment, we consider two samples of monodisperse CaO subjected to carbonation/decomposition cycles with different durations of the carbonation stage $T_1 = 7.5$ min and $T_2 = 30$ min at the same temperature 800°C. The duration of the decomposition stage was 30 min in all cases, which was sufficiently enough for entire decomposition of formed calcium carbonate. According to our model of the $CaCO_3$ layer growth, we assume that corresponding maximal thicknesses of the $CaCO_3$ layer relate as $d_2 = 2d_1$. Varying all parameters of the model under this assumption and utilizing the least squares method, we obtain a prediction of the RE presented in Fig. 7. Because of the lack of experimental data on the porosity of original CaO, we suppose that the CaO sample before the very first carbonation stage may have additional pores, which influences the additional decay of the RE during a first few cycles. To take this effect into account, we also vary the number of first cycles on which the model is applicable. As we see, the longer carbonation time provides a higher RE, so the thickness d in this case is more significant than the shrinkage factor.

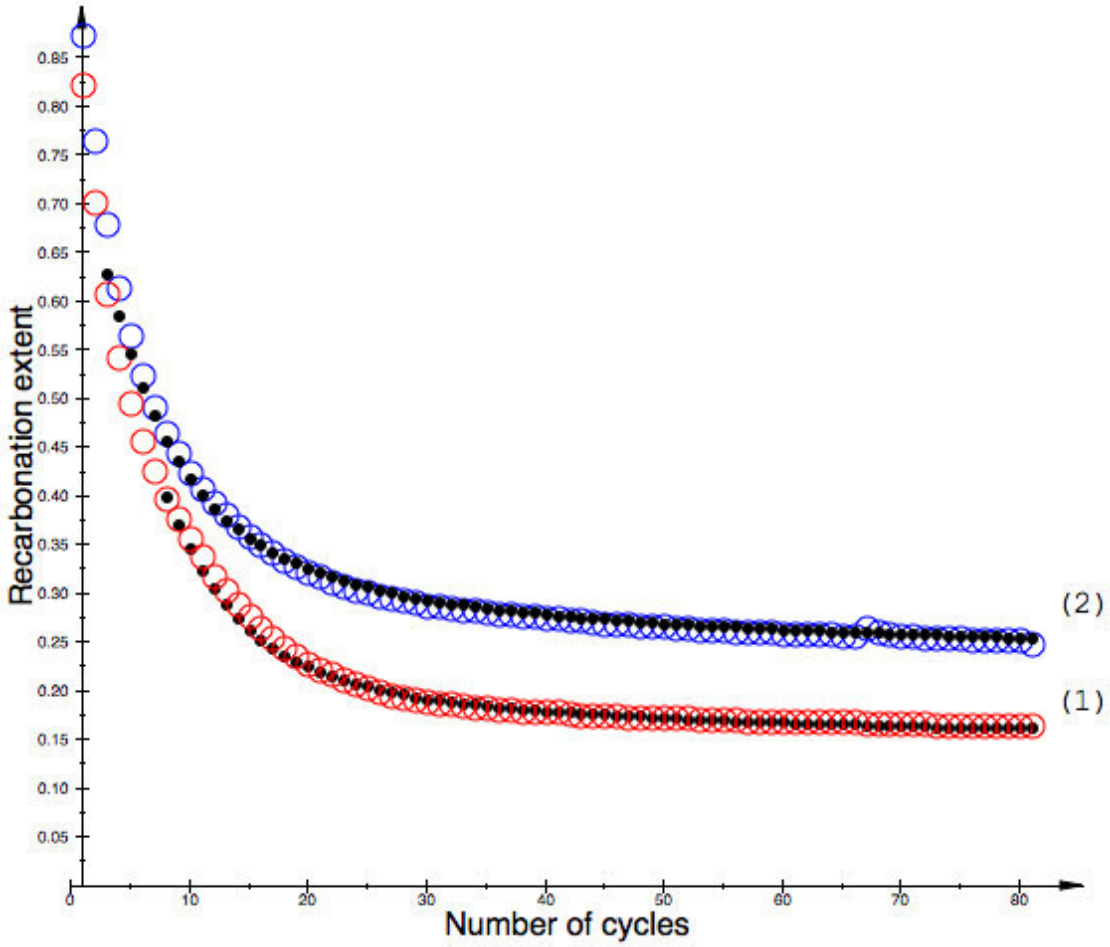

Figure 7. Recarbonation extent during carbonation/decomposition cycles with different carbonation times (1) $T_1 = 7.5$ min and (2) $T_2 = 30$ min at the same temperature 800°C. Large empty circles represent real experiment data; small filled circles represent prediction of the model. The limit shrinkage factors and percentage of the maximal thickness d with respect to the mean diameter of grains are the following: (1) $\mu_1 \approx 0.88, \delta_1 \approx 7\%$, (2) $\mu_2 \approx 0.80, \delta_2 \approx 11\%$.

In the second experiment, we begin with carbonation/decomposition cycles as described above and replace carbonation times after a sufficient number of cycles (81-84 cycles) until the RE becomes stable. This experiment demonstrates the influence of both the thickness and the shrinkage factor on the RE. Before switching of the carbonation mode, we see that the RE for the longer carbonation time $T_2 = 30$ min is higher than the RE for $T_1 = 7.5$ min, as discussed above. After the switching, we see that the new RE of sample (1) becomes lower than the RE of sample (2). Similarly, the RE of sample (2) after the change in carbonation time becomes higher than the RE of sample (1). We explain this effect as follows. At the longer carbonation time, the shrinkage factor is smaller (that is, longer T gives a more powerful sintering effect). Therefore, at the same d, a smaller μ gives a lower RE, and vice versa. This effect is presented in Fig. 8. At

the beginning of each phase after the switching of carbonation times, we see that the RE in the prediction curves changes instantly, while the real experimental curves have a delay effect. We can explain this effect with the local rearrangement of the layer structure [30] (for example, because of additional microporosity of grains), which we do not take into account in our model.

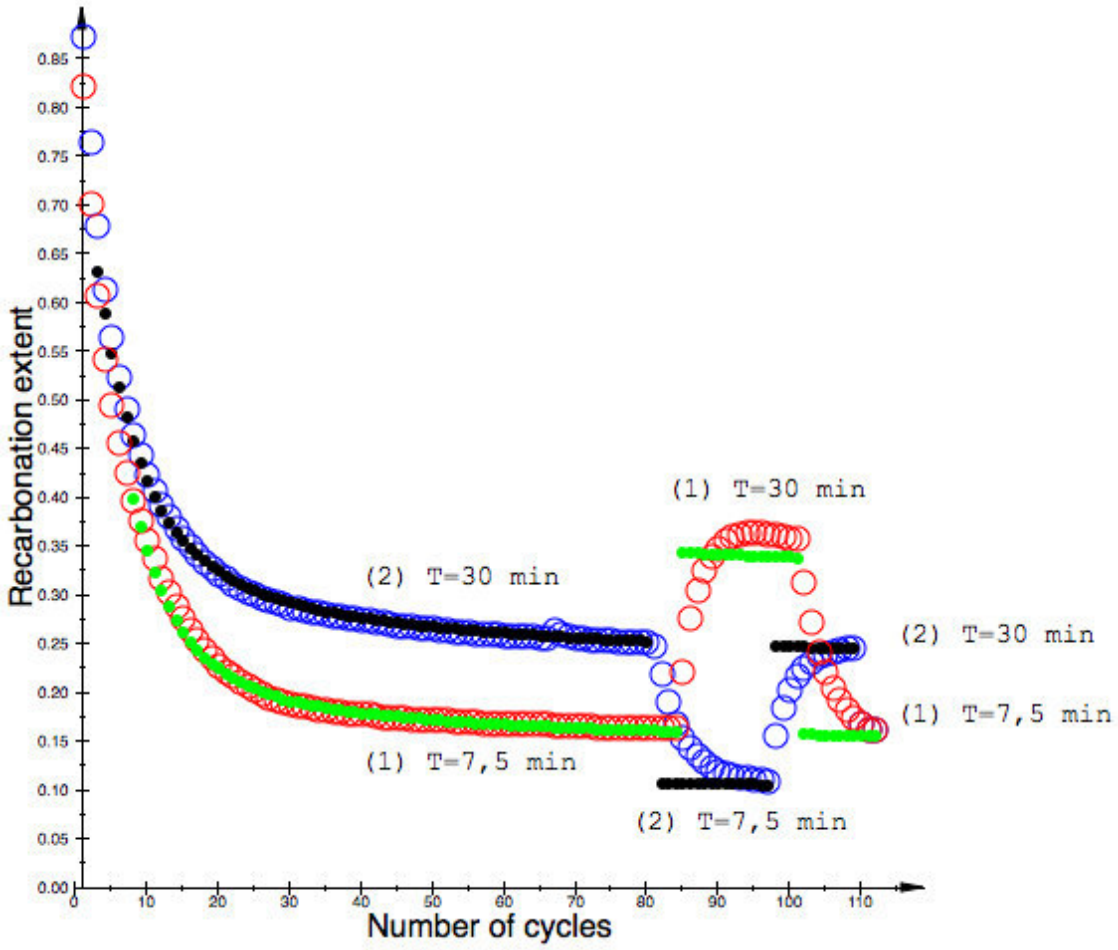

Figure 8. Recarbonation extent during carbonation/decomposition cycles with different carbonation times (1) $T_1 = 7.5$ min and (2) $T_2 = 30$ min at the same temperature 800°C. After approximately 81-84 cycles, we switched T_1 and T_2. After 105-110 cycles, we switched carbonation times again. Large empty circles represent real experiment data; small filled circles represent prediction of the model. The limit shrinkage factors and percentage of the maximal thickness d with respect to the mean diameter of grain are the following: (1) $\mu_1 \approx 0.88, \delta_1 \approx 7\%$, (2) $\mu_2 \approx 0.80, \delta_2 \approx 11\%$.

In the third experiment, we represent RE curves of the CaO granule with different carbonation/decomposition temperatures and with the same cycle times. All parameters of the

model were varied independently. We see in Fig. 9 that higher temperatures provide smaller shrinkage factors (and thus more intense sintering of grains), but the dependence of the thickness d on temperature in our model is rather unclear.

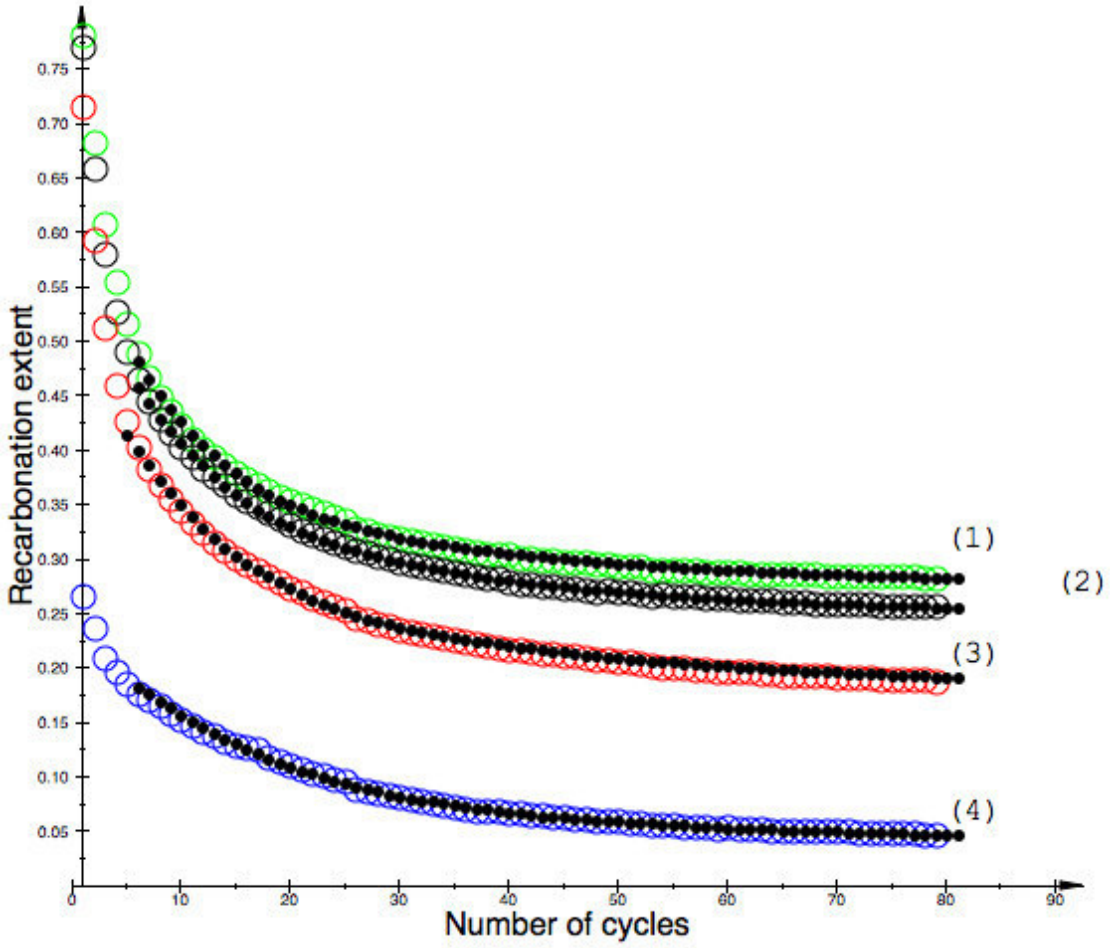

Figure 9. Recarbonation extent at different temperatures: (1) 750°C, $\mu = 0.91$; (2) 800°C, $\mu = 0.89$; (3) 822°C, $\mu = 0.87$; (4) 850°C, $\mu = 0.75$. Empty circles represent real experiment data; filled circles represent prediction of the model.

Several estimates [26,31,32] show that the thickness of the $CaCO_3$ layer depends greatly on the carbonation conditions and varies from 20 to 160 nm. Since the size of original CaO obtained from the SEM micrograph (Figure 2) was 500-800 nm and the percentage of the maximal thickness d with respect to the mean diameter of grains were 7% and 11%, respectively, the effective thickness of the $CaCO_3$ layer is 35-90 nm. Thus, our model predicts the thickness d that is comparable with experimental data.

4. CONCLUSION

In this study, the mathematical model for the repetitive sorption/regeneration cycling of CaO-based sorbent was proposed and tested. The obtained model takes into account the morphology of nascent CaO, the influence of the sorbent sintering and carbonation kinetics on the sorbent morphology and on the sorption capacity evolution in sorption/regeneration cycles. The structure of the material was modeled with the dense random packing of spheres using the Lubachevsky-Stillinger compression algorithm. The obtained resulted were compared with experimental data. The sintering was modeled under the following assumptions: the sintering proceeds via the lattice diffusion mechanism, and the sintering rate of $CaCO_3$ is higher than that of CaO. The obtained model allows predicting well the dependence of textural changes and the recarbonation extent on the number and duration of the sorption/regeneration cycles. The results show that the model is in good agreement with experimental data on repetitive sorption/regeneration cycles of real sorbents. A further improvement of the model, which would take in account the sorbent morphology in more detail, the dependence of sintering of CaO and its reactivity with CO_2 on temperatures and pressures, seems to be useful for making a universal model for determination of the CaO-based sorbent properties under various reaction conditions.

ACKNOWLEDGEMENT

Ya.V.Bazaikin acknowledges institutional support of University Hradec Kralove. The authors thank Dr. Aleksey Gladky for technical assistance and Anna Derevschikova for graphic design assistance.

AUTHOR INFORMATION

Corresponding Author *Email: derevshchikov@mail.ru

REFERENCES

(1) Karimi, F.; Khalilpour, R. *Int. J. Greenh. Gas Control* **2015**, *37*, 362–376.

(2) Lee, S.-Y.; Park, S.-J. *J. Ind. Eng. Chem.* **2015**, *23*, 1–11.

(3) Florin, N.; Fennell, P. *Energy Procedia* **2011**, *4*, 830–838.

(4) Bhatta, L. K. G.; Subramanyam, S.; Chengala, M. D.; Olivera, S.; Venkatesh, K. *J. Clean. Prod.* **2015**, *103*, 171–196.

(5) Angeli, S. D.; Martavaltzi, C. S.; Lemonidou, A. a. *Fuel* **2014**, *127*, 62–69.

(6) Hanak, D. P.; Biliyok, C.; Anthony, E. J.; Manovic, V. *Int. J. Greenh. Gas Control* **2015**, *42*, 226–236.

(7) Rodriguez, N.; Alonso, M.; Grasa, G.; Abanades, J. C. *Chem. Eng. J.* **2008**, *138*, 148–154.

(8) Di Felice, L. *CO2 Capture by CaO-Based Sorbents and Sorption Enhanced Reaction Systems*; Elsevier B.V., 2013.

(9) Abanades, J. C. *Chem. Eng. J.* **2002**, *90* (3), 303–306.

(10) Abanades, J. C.; Alvarez, D. *Energy and Fuels* **2003**, *17* (2), 308–315.

(11) Wang, J.; Anthony, E. J. *Ind. Eng. Chem. Res.* **2005**, *44* (3), 627–629.

(12) Grasa, G. S.; Abanades, J. C. *Ind. Eng. Chem. Res.* **2006**, *45* (26), 8846–8851.

(13) Lysikov, A. I.; Salanov, A. N.; Okunev, A. G. *Ind. Eng. Chem. Res.* **2007**, *46* (13), 4633–4638.

(14) Kierzkowska, A. M.; Pacciani, R.; Müller, C. R. *ChemSusChem* **2013**, *6*, 1130–1148.

(15) Sun, P.; Grace, J. R.; Lim, C. J.; Anthony, E. J. *AIChE Journal*. 2007, pp 2432–2442.

(16) German, R. M.; Munir, Z. a. *J. Am. Ceram. Soc.* **1976**, *59* (9-10), 379–383.

(17) Ushizima, D.; Morozov, D.; Weber, G. H.; Bianchi, A. G. C.; Sethian, J. a.; Bethel, E. W. *IEEE Trans. Vis. Comput. Graph.* **2012**, *18* (12), 2041–2050.

(18) Chen, Z.; Wang, X.; Giuliani, F.; Atkinson, A. *Acta Mater.* **2015**, *89*, 268–277.

(19) Lysikov, A. I.; Salanov, A. N.; Moroz, E. M.; Okunev, A. G. **2007**, *90* (1), 151–157.

(20) Lubachevsky, B. D.; Stillinger, F. H. *J. Stat. Phys.* **1990**, *60* (5-6), 561–583.

(21) Grasa, G. S.; Abanades, J. C.; Alonso, M.; González, B. *Chem. Eng. J.* **2008**, *137* (3), 561–567.

(22) Khawam, A.; Flanagan, D. R. *J. Phys. Chem. B* **2006**, *110* (35), 17315–17328.

(23) Wang, W.; Li, Y.; Xie, X.; Sun, R. *Appl. Energy* **2014**, *125*, 246–253.

(24) Bhatia, S. K.; Perlmutter, D. D. *AIChE J.* **1983**, *29* (1), 79–86.

(25) Suk-Joong L.Kang. *Elsevier Butterworth-Heinemann Linacre House* **2005**, No. ISBN 978-0-7506-6385-4., pp. 9–18.

(26) Alvarez, D.; Abanades, J. C. *Energy and Fuels* **2005**, *19* (1), 270–278.

(27) H. Borgwardt, R. *Chem. Eng. Sci.* **1989**, *44* (1), 53–60.

(28) Borgwardt, R. H. *Ind. Eng. Chem. Res.* **1989**, *28* (1961), 493–500.

(29) Geguzin, Y. E.; others. Nauka, Moscow 1967.

(30) Anthony, E. J. **2008**, *42* (11), 4170–4174.

(31) Sun, P.; Grace, J. R.; Lim, C. J.; Anthony, E. J. *Chem. Eng. Sci.* **2008**, *63* (1), 47–56.

(32) Alvarez, D.; Carlos Abanades, J. *Ind. Eng. Chem. Res.* **2005**, *44* (15), 5608–5615.

Рецензия на итоговый отчёт «Дизайн высокотемпературных регенерируемых сорбентов CO_2»

Развитый теоретический аппарат для описания процесса спекания частиц CaO достаточно сложен для понимания. Речь идёт о формулировке задачи Коши, дифференциальных уравнений и её итерационного решения.

Предполагается, что частицы CaO стягиваются силами *упругого натяжения* слоя $CaCO_3$. При этом, на каждую частицу CaO действует результирующая сила F, которая приводит в движение частицу с ускорением, согласно второму закону Ньютона. Эта самая сила, согласно работе авторов (выражение 16) есть:

$$F = \alpha R d$$

где α – коэффициент, названный удельной энергией объёма. По своему смыслу эта величина означает энергию, запасённую в результате сжатия. Её размерность, очевидно, Дж/м^3. Далее, R – коэффициент поверхностного натяжения, Дж/м^2. d – толщина слоя, м. Как при этом получается правильная размерность силы? Тут явно требуется комментарий, откуда было получено это выражение и каков смысл переменных.

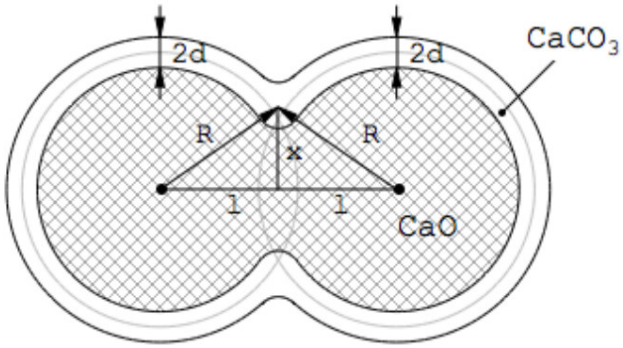

Figure 6. Sintering of two grains.

Рис. 1: Модель спекания двух частиц CaO.

Утверждается, что l изменяется согласно второму закону Ньютона, и мы имеем уравнение движения (20):

$$m\frac{d^2 l}{dt^2} = -(F - F_f)$$

где появляется так называемая сила $F_f = \sigma_0 (x-d)^2$, по смыслу, сила поверхностного натяжения зоны контакта частиц. С этого уравнения движения берёт начало развитый в работе математический аппарат.

В работе даётся ссылка на книгу Suk-Joong L. Kang // Sintering. Densification, Grain Growth, and Microstructure и книгу Я.Е. Гегузина «Физика спекания». В последней есть термин «капиллярное сжатие контактирующих частиц», однако, речь идёт, как и ожидалось, о слиянии капель, а не твердых частиц. Дифференциальное уравнение спекания в той форме, что предложена авторами, не встречается в цитированной литературе. Если это не так – хорошо, покажите те места в книгах.

В отчёте не отражены характерные массы, размеры частиц и времена спекания. Откуда взяты численные значения коэффициентов. Размерности. Просто куча формул и как кролик из шляпы фокусника – некий результат. Качество выполнения основной задачи проекта (номер 2 аннотации: «На базе экспериментальных данных построить адекватную математическую модель процессов сорбции – регенерации в пористой среде..»,) можно поставить под сомнение.